



Fabrication of $\text{Ag}_3\text{PO}_4/\text{TiO}_2$ Composite and Its Photodegradation of Formaldehyde Under Solar Radiation

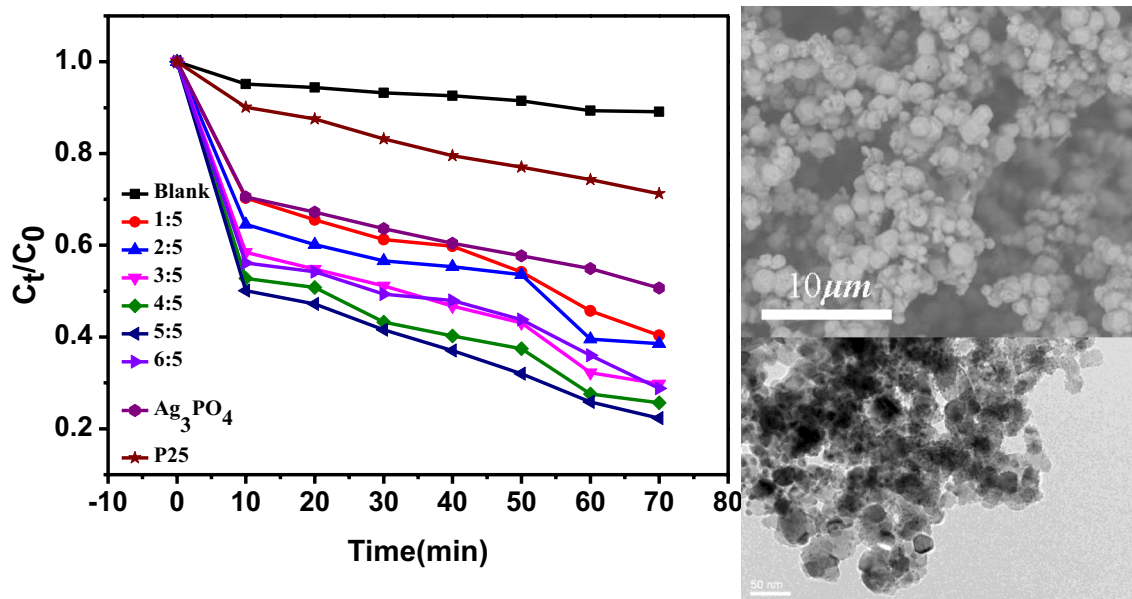
Lu Zhang¹ · Deyou Yu¹ · Minghua Wu^{1,2} · Junxiong Lin¹

Received: 29 June 2018 / Accepted: 4 January 2019 / Published online: 17 January 2019
© Springer Science+Business Media, LLC, part of Springer Nature 2019

Abstract

In order to improve the photocatalytic degradation performance of Ag_3PO_4 and reduce the cost of photocatalyst made of Ag_3PO_4 , a kind of $\text{Ag}_3\text{PO}_4/\text{TiO}_2$ composite was successfully fabricated via a simply precipitation method for the Ag_3PO_4 nanoparticles being loaded on the surface of commercial titanium dioxide (P25) to form a heterostructure. The $\text{Ag}_3\text{PO}_4/\text{TiO}_2$ composite were characterized by FT-IR, XRD, XPS, FE-SEM, HR-TEM, DRS and PL and applied for the degradation of formaldehyde solution under solar radiation. The results showed that the degradation rate of $\text{Ag}_3\text{PO}_4/\text{TiO}_2$ composite (0.01796 min^{-1}) was much higher than that of pure Ag_3PO_4 (0.00775 min^{-1}), indicating that the $\text{Ag}_3\text{PO}_4/\text{TiO}_2$ composite possessed better photocatalytic degradation activity for the formaldehyde solution than pure Ag_3PO_4 . The composite significantly decreased the dosage of silver for photocatalyst under solar radiation, thereby reduced the cost of the photocatalyst made from silver.

Graphical Abstract



Keywords Ag_3PO_4 · $\text{Ag}_3\text{PO}_4/\text{TiO}_2$ composite · Photocatalytic formaldehyde

✉ Minghua Wu
wmh@zstu.edu.cn

Extended author information available on the last page of the article

1 Introduction

With the development of economy and the improvement of people's living standard, the interior decoration was paid more attention, and lots of textiles were used. This inevitably results in indoor air pollution, among which formaldehyde is one of the most typical pollutants, and it is harmful to human body, prolonged exposure to formaldehyde may cause the immune system of body being injured, leading to central nervous system being damaged, growth disorders, blindness and respiratory diseases [1, 2], and may even cause cancer and probably leukemia [3]. It is urgent to remove formaldehyde efficiently, and to do it without secondary pollution.

Photocatalytic technology widely used as a kind of green technology in energy conversion, pollution treatment and air purification has attracted great attention in recent years. Among the numerous semiconductor photocatalysts, silver phosphate (Ag_3PO_4), a kind of materials with quantum efficiency up to 90% [4, 5], which can absorb sunlight with wavelength short than 520 nm [6], has been widely researched for its extremely high photooxidative capabilities for O_2 evolution from water as well as the degradation of organic pollutants under visible light irradiation [7]. As a kind of narrow band gap photocatalysts [8], Ag_3PO_4 , with higher photocatalytic activity than that of many other visible light photocatalysts such as TiO_2-xN_x , BiVO_4 and WO_3 [9], has a wide range of applications in the future. However, the silver belongs to noble metal, its price is relatively high. How to reduce the cost of its application without sacrificing its photocatalytic performance is still a challenge.

The titanium dioxide (TiO_2) has been proved to be a prospect photocatalysts because of its low cost, nontoxicity and long-term photostability [10–13]. But the band gap of TiO_2 is large, which makes it only absorb the lights in ultraviolet (UV) region. While the UV light occupied only 3–5% in the solar spectrum, this may limited the application of TiO_2 in visible region [14]. To improve the utilization ratio of solar light, much efforts has been invested to expand the band gap of TiO_2 , including metal and non-metal ion doping [14], organic dye sensitization, surface precious metal deposition, semiconductor composite and other means [15]. Obviously, the semiconductor composite has proved to be an efficient way to extend the absorption spectra of TiO_2 into the visible region [16–19].

However, the conduction band of TiO_2 is more negative than that of Ag_3PO_4 , and the valence band of them are similar [20, 21], thus it is appropriate to construct heterojunction to make the composite response under visible light and reduce the cost of the photocatalyst made from silver [22]. Therefore, in this study, we use a simple

precipitation method by depositing Ag_3PO_4 nanoparticles onto the surface of commercial TiO_2 (P25) to prepare the $\text{Ag}_3\text{PO}_4/\text{TiO}_2$ composite for reducing the cost of the photocatalysts made from silver while not affecting its photocatalytic property. Taking into account the convenience of the experiments, the composites were applied to degrade formaldehyde in aqueous solution, the photocatalytic property of the composite has been measured, and compared with that of pure Ag_3PO_4 and P25.

2 Experimental

2.1 Materials

Silver nitrate (AgNO_3), formaldehyde solution (HCHO), isopropanol (IPA) and ammonia ($\text{NH}_3\cdot\text{H}_2\text{O}$) were obtained from Hangzhou Gaojing Fine Chemical Co. Ltd. Sodium hydrogen phosphate ($\text{Na}_2\text{HPO}_4\cdot 12\text{H}_2\text{O}$), ethylene diamine tetraacetic acid (EDTA) and benzoquinone (BQ) were purchased from Aladdin Reagent Co. Ltd. These above reagents were all analytical grade. Commercial titanium dioxide (P25, mixture of anatase and rutile) was achieved from Guangzhou Heqian Trading Co. Ltd. All of the experiments the deionized water were used. The reagents were used as received without further purification.

2.2 The Fabrication of $\text{Ag}_3\text{PO}_4/\text{TiO}_2$ Composite

The $\text{Ag}_3\text{PO}_4/\text{TiO}_2$ composite was fabricated by a simple precipitation method as following: 0.005 mol commercial TiO_2 was dispersed in 30 mL deionized water to form a mixture, and the pH of the mixture was adjust to 10 with ammonia, then the mixture was sonicated for 20 min to obtain a white suspension. Subsequently a certain amount of AgNO_3 (0.1 M) was added into the suspension, which was continuously stirred for 30 min. Then the Na_2HPO_4 (0.1 M) solution was added dropwise into the above solution, which was stirred for 5 h at room temperature. After that, the precipitate was obtained by centrifugated and rinsed thoroughly with deionized water until the solution near neutral, and it was dried in the vacuum at the temperature of 60 °C for 12 h. Finally the $\text{Ag}_3\text{PO}_4/\text{TiO}_2$ composite was obtained. For comparison, the pure Ag_3PO_4 was obtained at the same conditions in the absence of commercial TiO_2 .

2.3 Characterizations

Fourier transform infrared (FT-IR) analysis was performed to evaluate the functional identification of the composite photocatalysts using a spectrophotometer (Nicolet iS50, USA) in a wavenumber ranging from 400 to 4000 cm^{-1} . X-ray diffraction (XRD) patterns were identified by a ARL

XTRA diffractometer (Thermo ARL, Switzerland) to record the crystal structures over 2θ in the range of 20° – 80° at a scanning rate of $4^\circ/\text{min}$. X-ray photoelectron spectroscopy (XPS) was conducted on a K-Alpha spectrometer (Thermo Fisher Scientific, USA) to detect the chemical states and the elemental composition of the composite, and the binding energy was calibrated by the C1s peak of the contamination carbon. The surface morphology structure of the composite photocatalysts was observed by the Field emission scanning electron microscope (JSM-5610LV, JEOL, Japan). The lattice structure of the sample was examined by the high-resolution Transmission electron microscopy (GATAN, 832, USA). The diffuse reflectance spectra (DRS) was recorded on a UV–Vis spectrophotometer in the wavelength range of 325–700 nm. The photoluminescence spectroscopy (PL) was obtained by using the fluorescence spectrophotometer (F-46001, Japan). The electron spin resonance (ESR) signals of superoxide radical ($\cdot\text{O}_2^-$) and hydroxyl radical ($\cdot\text{OH}$) trapped by DMPO were conducted by a Bruker model spectrophotometer.

2.4 Photocatalytic Degradation Test

The photocatalytic activity of all samples was measured by the decomposition of formaldehyde solution in a reactor at room temperature during the process by circulating with cool water, with a 350 W xenon lamp as light source, 100 mg $\text{Ag}_3\text{PO}_4/\text{TiO}_2$ composite was dispersed in 50 mL the as-prepared formaldehyde solution (3.2 mg/L), and before the photocatalytic reaction, first the suspension was stirred in the dark condition for 30 min for adsorption–desorption equilibrium, then, under the light source, the photocatalytic reaction experiment was carried out. Take 5 mL of the reaction liquid at any given time, then the reaction liquid was centrifugated to get the supernatant, the as-prepared acetylacetone solution

which used as the colour reaction agent of the formaldehyde solution was added into the supernatant to get a pale yellow transparent solution. According to the change of the absorbance at the maximum absorption wavelength (413 nm), the change of the concentration of formaldehyde solution was determined, so as to judge the photocatalytic degradation performance of the photocatalyst. The residual rate of the solution was calculated by $R = \{1 - (C_0 - C_t)/C_0\} \times 100\%$, where C_0 and C_t were the concentrations of the solution, when the reaction time was 0 and t respectively. According to the Langmuir–Hinshelwood kinetics model, the process of the photocatalytic reaction in accordance with first-order kinetics can be expressed as the following equation [23]:

$$-\ln(C_t/C_0) = k_{\text{app}}t.$$

3 Results and Discussion

3.1 Structure and Morphology Analysis of $\text{Ag}_3\text{PO}_4/\text{TiO}_2$ Composite

The infrared spectra of Ag_3PO_4 and $\text{Ag}_3\text{PO}_4/\text{TiO}_2$ composite photocatalysts were showed in Fig. 1. These infrared spectra were ranged from 400 to 4000 wavenumbers. Figure 1a shows two board peaks, the board peak around 3000 cm^{-1} was assigned to the O–H stretching vibration of the adsorbed water, the peak around 975 cm^{-1} can be assigned to the PO_4^{3-} stretching vibration [24], and compared with Fig. 1a, there were another two peaks in Fig. 1b, they are around 700 and 1100 cm^{-1} , the board peak corresponds to the O–Ti–O bond stretching. Therefore the infrared spectra indirectly proved that the $\text{Ag}_3\text{PO}_4/\text{TiO}_2$ composite photocatalysts had been achieved.

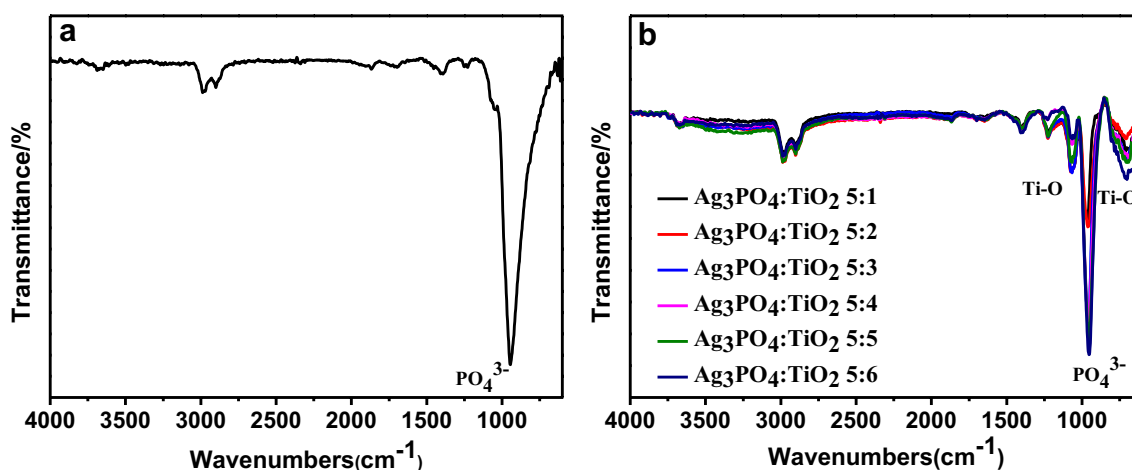


Fig. 1 The infrared spectra of **a** Ag_3PO_4 and **b** $\text{Ag}_3\text{PO}_4/\text{TiO}_2$ composite

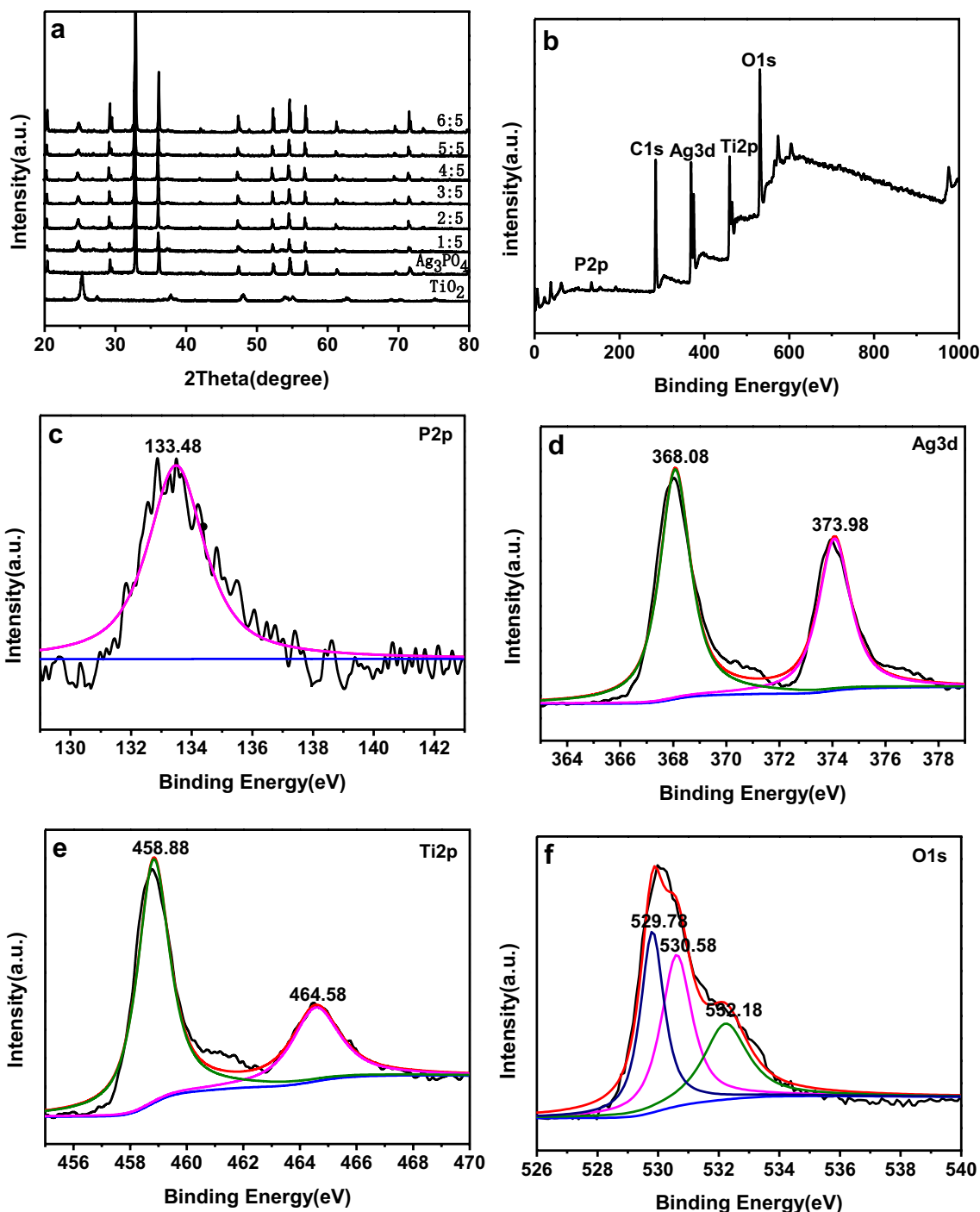


Fig. 2 a XRD patterns of TiO_2 , as-prepared Ag_3PO_4 and $\text{Ag}_3\text{PO}_4/\text{TiO}_2$ composite, b–f The XPS spectrum of the $\text{Ag}_3\text{PO}_4/\text{TiO}_2$ composite, in which b survey spectrum, c P 2p, d Ag 3d, e Ti 2p, f O 1s

Figure 2a shows the XRD patterns of commercial TiO_2 (P25), as-prepared Ag_3PO_4 and $\text{Ag}_3\text{PO}_4/\text{TiO}_2$ composite. It is observed that the XRD pattern of Ag_3PO_4 was in good agreement with the XRD pattern of the standard Ag_3PO_4 (JCPDS no. 06-0505) [22], it was attributed to the body-centered cubic structure, the diffraction peak was sharp, and

the half peak width was narrow, there was no impurity peak, it showed that Ag_3PO_4 has higher crystallinity and fewer crystal defects. The titanium dioxide was commercial TiO_2 (P25), a mixture of anatase and rutile phase. The $\text{Ag}_3\text{PO}_4/\text{TiO}_2$ composite showed the characteristic diffraction peaks of Ag_3PO_4 and TiO_2 , there were no other impurity peaks, the

result revealed that there was no chemical reaction between Ag_3PO_4 and P25.

In order to further analysis the chemical states and the elemental composition of the composite, XPS measurements were carried out, and the result can be seen in Fig. 2b–f. From the survey spectrum the primarily peaks are correspond to Ti, O, Ag, C and P elements. The element of carbon was attributed to the calibration carbon. The peak centered at 133.48 eV was related to the p^{5+} of P 2p in Ag_3PO_4 [25], and from the picture the peaks at 368.08 eV and 373.98 eV were seen which were corresponded to the $3\text{d}_{3/2}$ and $3\text{d}_{5/2}$ of Ag^+ respectively [26], there was no peak found at 369.2 eV and 375.8 eV which proved that there is no Ag^0 exist. The peak located at 458.88 eV and 464.58 eV could be assigned to Ti $2\text{p}_{1/2}$ and Ti $2\text{p}_{3/2}$ respectively [20], and the splitting between them is 5.7 eV, indicating that the element of Ti was in the normal state of Ti^{4+} . The element of oxygen have three different forms of binding energy on the surface of the composite, they were 529.78 eV, 530.58 eV and 532.18 eV respectively, and the peaks at 529.78 eV and 530.58 eV were attributed to the oxygen lattices in Ag_3PO_4 and TiO_2 [27], the other one was ascribed to the present of hydroxyl groups on the surface of the composite. The results of XPS further proved that we had obtained the $\text{Ag}_3\text{PO}_4/\text{TiO}_2$ composite.

Figure 3a showed the morphological characteristics of the $\text{Ag}_3\text{PO}_4/\text{TiO}_2$ composite when the molar ratio of Ag_3PO_4 and TiO_2 was 5:5. From the image, it could be seen that there were two kinds of particles (big particles and small particles), and the smaller nanoparticles were loading on the surface of the bigger one. Figure 3b, c show the TEM images of TiO_2 and $\text{Ag}_3\text{PO}_4/\text{TiO}_2$ composite. For further observation, Fig. 3d showed the high magnification TEM image of $\text{Ag}_3\text{PO}_4/\text{TiO}_2$ composite. The image of Fig. 3b revealed that the average particle size of TiO_2 was about 25 nm, and from the image of Fig. 3d it could be seen clearly that there were two types of lattice fringes. One of the observed lattice spacing of 0.350 nm was in good agreement with the (101) plane of anatase TiO_2 (JPCDS no. 21-1272) [21], and the other lattice spacing of 0.268 nm was attributed to the (210) plane of Ag_3PO_4 (JPCDS no. 06-0505) [22]. Therefore it can be conclude that the Ag_3PO_4 nanoparticles were successfully loading on the surface of TiO_2 , and the TEM image was shown in Fig. 3c, the size of these Ag_3PO_4 nanoparticles was about 5–9 nm, it was much smaller than that of pure Ag_3PO_4 with the average particle size being about 1261 nm. This may be due to the electrostatic repulsion between TiO_2 and HPO_4^- , which slowed the reaction between Ag^+ and

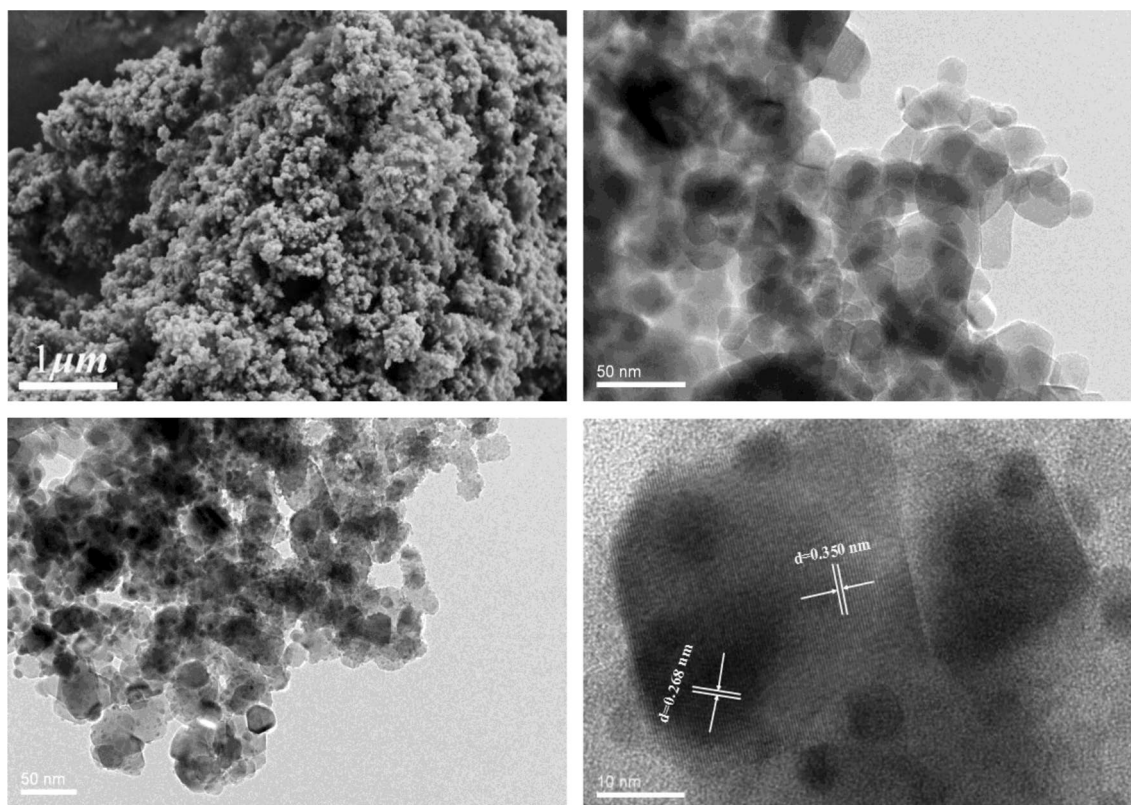


Fig. 3 a SEM image of $\text{Ag}_3\text{PO}_4/\text{TiO}_2$ composite ($\text{Ag}_3\text{PO}_4:\text{TiO}_2$ 5:5), b, c TEM images of TiO_2 and $\text{Ag}_3\text{PO}_4/\text{TiO}_2$ composite ($\text{Ag}_3\text{PO}_4:\text{TiO}_2$ 5:5), d HR-TEM image of $\text{Ag}_3\text{PO}_4/\text{TiO}_2$ heterostructures

PO_4^{3-} , therefore, the size of Ag_3PO_4 on the surface of TiO_2 was relatively small.

The UV–Vis diffuse reflectance spectroscopy of Ag_3PO_4 , commercial TiO_2 and $\text{Ag}_3\text{PO}_4/\text{TiO}_2$ composite were shown in Fig. 4. It could be seen clearly that TiO_2 could only absorb the light in UV region, barely absorb the light in visible light region. The UV–Vis diffuse reflectance spectroscopy of Ag_3PO_4 indicates that it could absorb the solar energy with the absorption edge about 506 nm. From the picture it could be observed that the $\text{Ag}_3\text{PO}_4/\text{TiO}_2$ composite showed a red shift in its absorption bands being compared with TiO_2 , and it had a strong absorption in solar, which was because of the Ag_3PO_4 nanoparticles loading on the surface of TiO_2 to form a heterostructure.

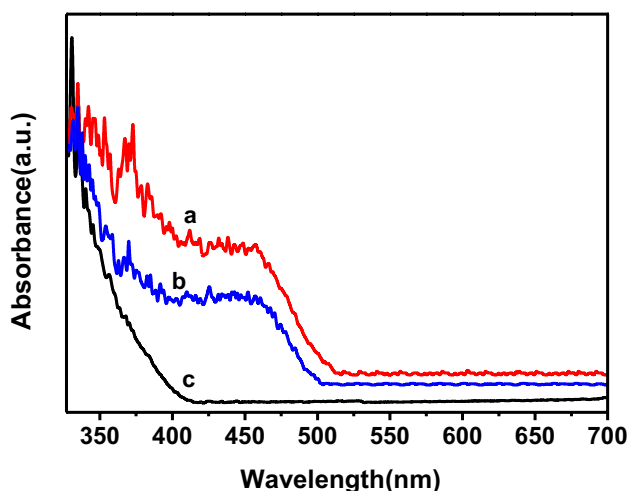


Fig. 4 UV–Vis absorption spectra of **a** Ag_3PO_4 , **b** $\text{Ag}_3\text{PO}_4/\text{TiO}_2$ composite ($\text{Ag}_3\text{PO}_4:\text{TiO}_2$ 5:5) and **c** the commercial TiO_2

3.2 Photocatalytic Degradation Performance Test Under Solar Radiation

The photocatalytic degradation performance of $\text{Ag}_3\text{PO}_4/\text{TiO}_2$ composite were shown in Fig. 5. To silver phosphate, after solar radiation for 70 min, almost 50% of the formaldehyde had been degraded, this proved that silver phosphate had a certain extent capability of degrading formaldehyde solution, but it is not ideal, and the silver belonged to noble metal, its price is relatively high. In this article, the cheaper TiO_2 was chosen to composite with Ag_3PO_4 for reducing the dosage of Ag_3PO_4 for preparing photocatalyst, and it was found that the $\text{Ag}_3\text{PO}_4/\text{TiO}_2$ composite had a better photocatalytic activity compared with Ag_3PO_4 as photocatalyst, after solar radiation for 70 min almost 80% of the formaldehyde could be degraded. With the increase of Ag_3PO_4 in the composite, the photocatalytic activity increase, especially when the molar ratio of Ag_3PO_4 and TiO_2 was 5:5, the degradation rate (0.01796 min^{-1}) of formaldehyde over $\text{Ag}_3\text{PO}_4/\text{TiO}_2$ are 2.32 times higher than that (0.00775 min^{-1}) of Ag_3PO_4 , when the Ag_3PO_4 being increased continuously the photocatalytic activity of $\text{Ag}_3\text{PO}_4/\text{TiO}_2$ composite decrease. For further analysis the photocatalytic activity of the photocatalysts, the PL spectrum analysis was carried out to investigate the separation efficient of photogenerated electrons and holes. Generally speaking, the lower PL emission signal indicates the higher separation efficient of photogenerated electrons and holes, and resulting in higher photocatalytic activity. The PL emission of TiO_2 , Ag_3PO_4 and $\text{Ag}_3\text{PO}_4/\text{TiO}_2$ composite was shown in Fig. 6. Compared with pure TiO_2 and Ag_3PO_4 , the PL intensity of $\text{Ag}_3\text{PO}_4/\text{TiO}_2$ composite decreased significantly, this clearly reveal that the Ag_3PO_4 composite with TiO_2 can obtain a higher charge separation efficiency, and the Ag_3PO_4 deposited on the surface of TiO_2 can greatly inhibited the recombination of

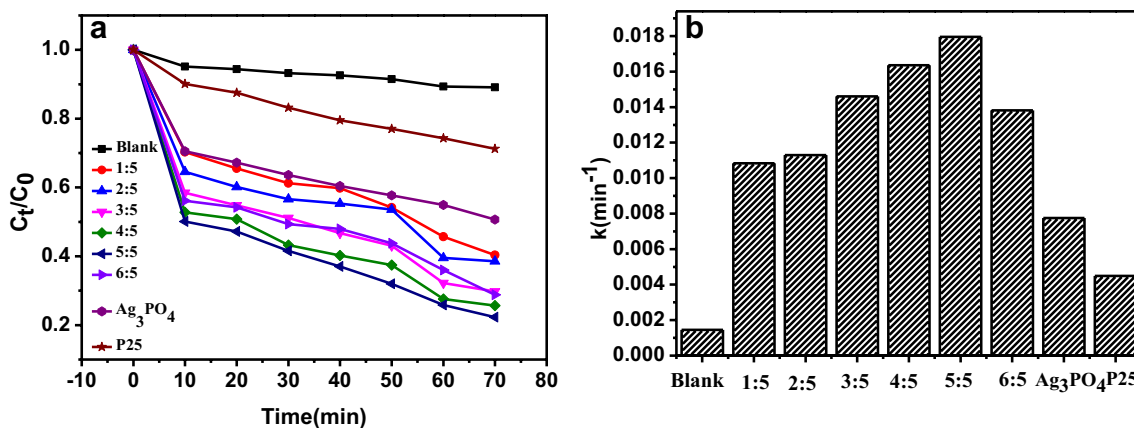


Fig. 5 **a** Photocatalytic activities of P25, Ag_3PO_4 and $\text{Ag}_3\text{PO}_4/\text{TiO}_2$ composite for the degradation of formaldehyde solution under solar radiation, **b** the apparent pseudo-first-order rate constant k_{app} of photocatalyst for the degradation of formaldehyde solution

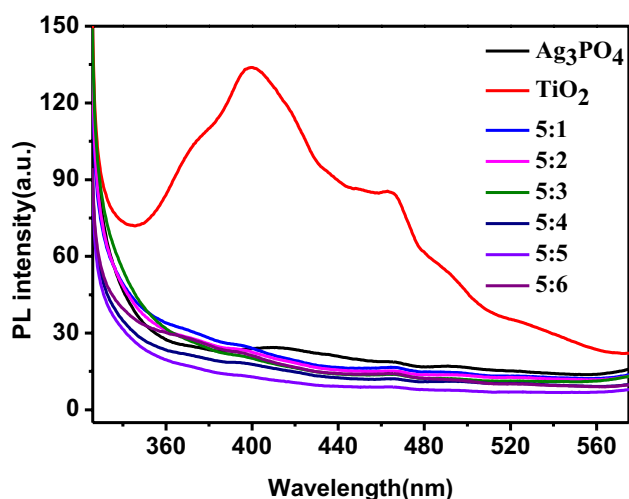


Fig. 6 PL spectrum of TiO_2 , Ag_3PO_4 and $\text{Ag}_3\text{PO}_4/\text{TiO}_2$ composite

photogenerated electrons and holes under solar radiation. The PL intensity decreased with the increase of Ag_3PO_4 being loaded on the surface of TiO_2 and reach a minimum when the molar ratio of Ag_3PO_4 and TiO_2 was 5:5, which indicating the better photocatalytic activity of the $\text{Ag}_3\text{PO}_4/\text{TiO}_2$ composite. However, the intensity of PL increased when the Ag_3PO_4 being increased continuously. This may be ascribed to the factor that the spare Ag_3PO_4 become the recombination centre of photogenerated electrons and holes. The PL results were in consistent with the photocatalytic activity of the $\text{Ag}_3\text{PO}_4/\text{TiO}_2$ composite.

3.3 Stability of $\text{Ag}_3\text{PO}_4/\text{TiO}_2$ Composite in Recycling Reaction for Formaldehyde Degradation

Apart from the photocatalytic degradation performance, the recycling stability of photocatalyst is another important performance for the practical application. The recycling experiments were carried out to compare the stability between $\text{Ag}_3\text{PO}_4/\text{TiO}_2$ composite and pure Ag_3PO_4 for the photodegradation of formaldehyde solution under solar radiation, as shown in Fig. 7. After three recycling runs, from the corresponding results we can know that the photocatalytic degradation performance of $\text{Ag}_3\text{PO}_4/\text{TiO}_2$ composite was better than pure Ag_3PO_4 in all these recycling experiments. The photocatalytic activity of Ag_3PO_4 and $\text{Ag}_3\text{PO}_4/\text{TiO}_2$ composite were all only slightly reduced after three consecutive recycling experiments, indicating that the combination of Ag_3PO_4 and TiO_2 didn't affect the cyclic stability of the composite. At the same time, the results indicate that the $\text{Ag}_3\text{PO}_4/\text{TiO}_2$ composite photocatalyst has a better photocatalytic activity and recycle stability compared with Ag_3PO_4 .

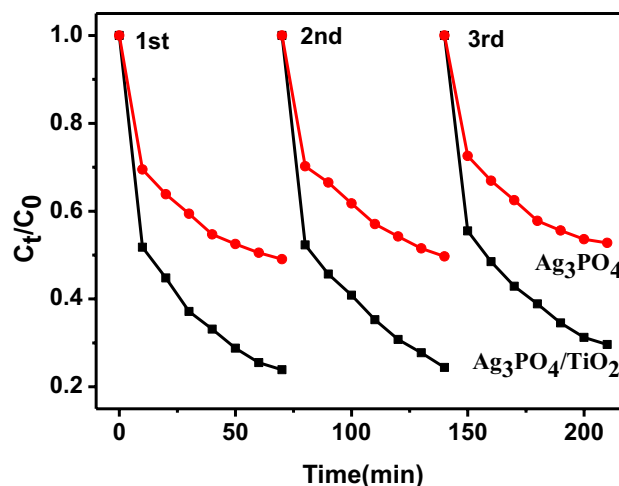


Fig. 7 Cyclic stability of Ag_3PO_4 and $\text{Ag}_3\text{PO}_4/\text{TiO}_2$ composite for the photodegradation of formaldehyde solution under solar radiation

3.4 The Mechanism of Photocatalytic Activity of $\text{Ag}_3\text{PO}_4/\text{TiO}_2$ Composite

In the process of photocatalytic reaction, the main factor that affects the activity of the photocatalysts is the separation and transfer of the photogenerated electrons (e^-) and holes (h^+). The photogenerated electrons tend to combine with O_2 in the solution to form superoxideradical ($\cdot\text{O}_2^-$), and the holes tend to combine with water molecules and hydroxyl ion to produce hydroxyl radical ($\cdot\text{OH}$). In order to study the mechanism of the degradation process, the scavenging experiments were conducted on $\text{Ag}_3\text{PO}_4/\text{TiO}_2$ composite which the mole ratio of Ag_3PO_4 and TiO_2 was 5:5 for the degradation of formaldehyde solution under solar radiation. In this study, three different chemicals ethylene diamine tetraacetic acid (EDTA), benzoquinone (BQ) and isopropanol (IPA) was used as scavengers for holes (h^+), superoxideradical ($\cdot\text{O}_2^-$) and hydroxyl radical ($\cdot\text{OH}$) respectively. As shown in Fig. 8a, b, it can be found that the photocatalytic degradation rate decreased in the order for decrease degree: IPA ($\cdot\text{OH}$) < BQ ($\cdot\text{O}_2^-$) < EDTA (h^+), when IPA was added in, the photocatalytic activity was slightly decreased, which indicate that $\cdot\text{OH}$ was not the main reactive species during the photocatalytic reaction. On the contrary, when EDTA and BQ were added in, the photocatalytic activity was significantly decreased, which indicated that h^+ and $\cdot\text{O}_2^-$ were the main reactive species during the photocatalytic reaction in the $\text{Ag}_3\text{PO}_4/\text{TiO}_2$ system. Furthermore, the main photocatalytic activity species $\cdot\text{OH}$ and $\cdot\text{O}_2^-$ of the $\text{Ag}_3\text{PO}_4/\text{TiO}_2$ composite were also detected by ERS spin-trap technique (with DMPO), as shown in Fig. 8c, d, there are six characteristic peaks of the DMPO- $\cdot\text{O}_2^-$ radicals under solar radiation that can not be detected under dark, and there is hardly

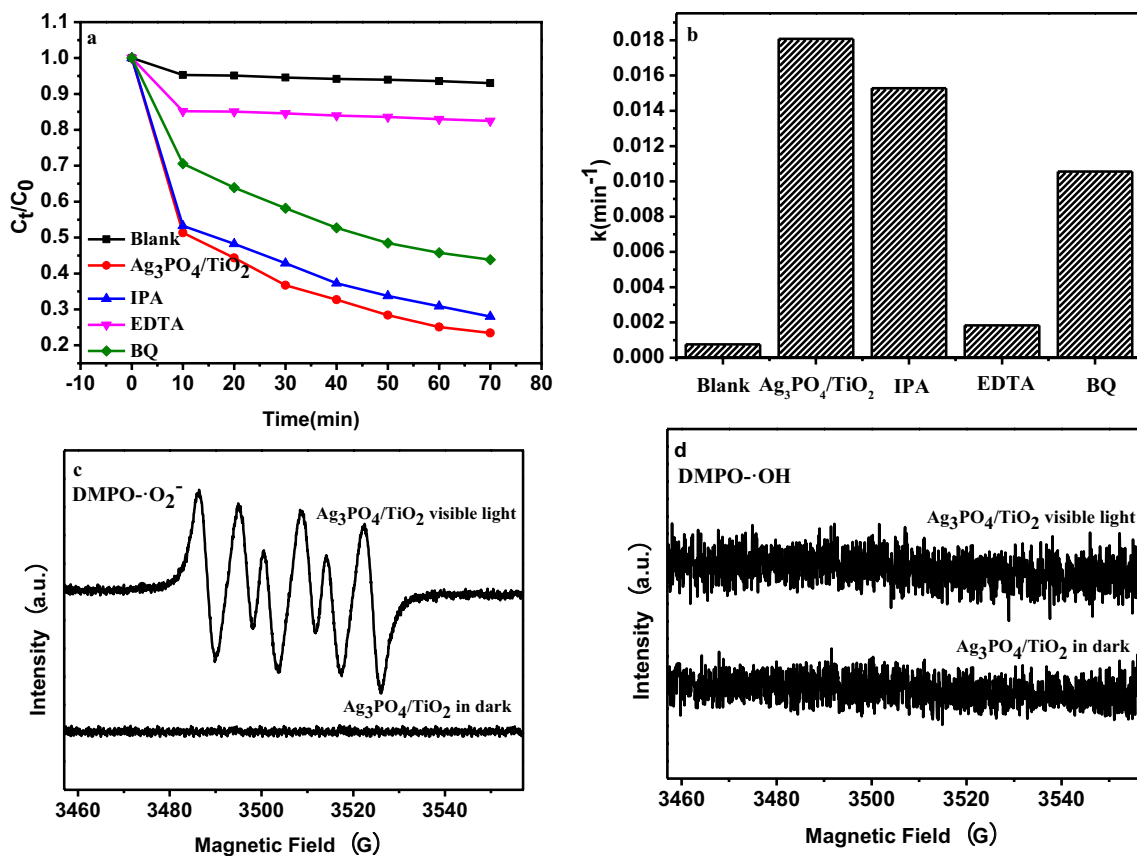


Fig. 8 **a** Photocatalytic activities of $\text{Ag}_3\text{PO}_4/\text{TiO}_2$ composite for the degradation of formaldehyde solution in the presence of different scavengers under solar radiation, **b** the apparent pseudo-first-order rate constant k_{app} with $\text{Ag}_3\text{PO}_4/\text{TiO}_2$ composite in the presence of

different scavengers for the degradation of formaldehyde solution, DMPO spin-trapping ESR spectra of $\text{Ag}_3\text{PO}_4/\text{TiO}_2$ composite photocatalytic $\text{c}\cdot\text{O}_2^-$ and **d** $\cdot\text{OH}$

any peak of the DMPO- $\cdot\text{OH}$ radicals whether under solar radiation or dark. Thus, h^+ and $\cdot\text{O}_2^-$ can be considered as the main reactive specie rather than $\cdot\text{OH}$ in $\text{Ag}_3\text{PO}_4/\text{TiO}_2$ composite photocatalytic reactions.

The probably mechanism of photocatalytic activity of $\text{Ag}_3\text{PO}_4/\text{TiO}_2$ composite was showed in Fig. 9. As shown in Fig. 9, under solar radiation, the Ag_3PO_4 and TiO_2 absorbed the photons, produced the photo-generated electrons in the conduction band (CB) and photo-generated holes in the valence band (VB), because of the potential valence band and conduction band of TiO_2 were more negative than that of Ag_3PO_4 [7, 28], then photo-generated holes quickly transferred to the surface of TiO_2 , photo-generated electrons transferred to the surface of Ag_3PO_4 , at the same time the photo-generated electrons absorbed O_2 in the solution to form $\cdot\text{O}_2^-$, in such a way, prevented the recombination of the photo-generated electrons and photo-generated holes to promote the separation of them, thus improved the photocatalytic activity of the $\text{Ag}_3\text{PO}_4/\text{TiO}_2$ composite photocatalyst.

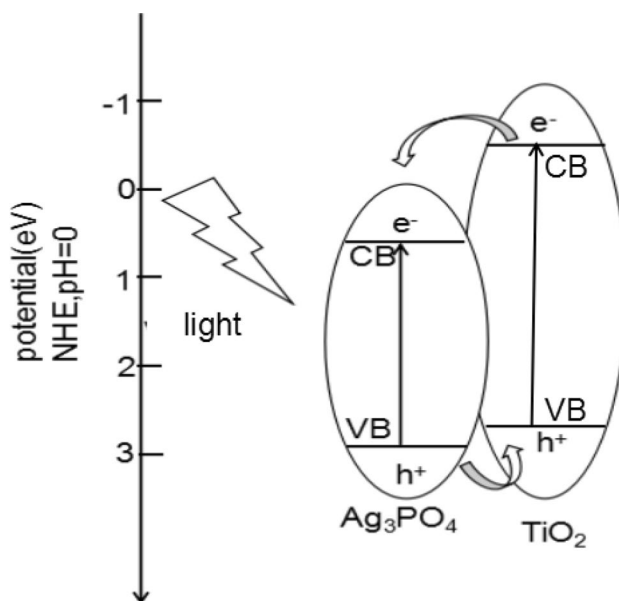


Fig. 9 The mechanism sketch map of photocatalytic reaction over the $\text{Ag}_3\text{PO}_4/\text{TiO}_2$ composite under solar radiation

4 Conclusion

The $\text{Ag}_3\text{PO}_4/\text{TiO}_2$ composite was successfully fabricated via a simply precipitation method. The Ag_3PO_4 nanoparticles were loaded on the surface of commercial titanium dioxide (TiO_2), and the size of Ag_3PO_4 nanoparticles was about 5–9 nm. From the images of the HR-TEM it could be seen that Ag_3PO_4 were dispersed on the surface of TiO_2 to form the formation of heterojunctions. The Ag_3PO_4 nanoparticles on the surface of TiO_2 made the absorption bands of TiO_2 have a red shift, thus improved the photocatalytic performance of the composite. The composite showed much higher photocatalytic activity under solar radiation than pure Ag_3PO_4 and TiO_2 for $\text{Ag}_3\text{PO}_4/\text{TiO}_2$ composite was a formation of heterojunctions. Therefore it was showed that the Ag_3PO_4 composited with TiO_2 can not only enhance the photocatalytic activity, but also reduce the cost of Ag_3PO_4 as photocatalyst under solar radiation.

Acknowledgements This study was kindly supported by Key Research and Development Program of Science and Technology Department of Zhejiang Province (NO. 2018C03004).

References

1. Ensafi AA, Honarmand E (2005) *Anal Sci* 21(5):545
2. Jones SB, Terry CM, And TEL (1999) *Anal Chem* 71(18):4030
3. Tang X, Bai Y, Duong A (2009) *Environ Int* 35(8):1210
4. Yan T, Guan W, Li W (2014) *RSC Adv* 4(70):37095
5. Guo X, Chen C, Yin S (2015) *J Alloys Compd* 619:293
6. Hua X, Jin Y, Wang K (2014) *Catal Commun* 52(8):49
7. Yi Z, Ye J, Kikugawa N (2010) *Nat Mater* 9(7):559
8. Zhao FM, Pan L, Wang S (2014) *Appl Surf Sci* 317:833
9. Vu TA, Dao CD, Hoang TT T (2013) *Mater Lett* 92(1):57
10. Lim YWL, Tang Y, Cheng YH (2010) *Nanoscale* 2(12):2751
11. Fujishima A, Honda K (1972) *Nature* 37(1):238
12. Ohno T, Sarukawa K, Tokieda K (2001) *J Catal* 203(1):82
13. Pan L, Zhang J, Jia Xu, Ma Y-H, Zhang X, Wang L, Zou J-J (2017) *Chin J Catal* 38(2):253
14. Cong Y, Zhang J, Chen F (2007) *J Phys Chem C* 111(19):6976
15. Yu J, Dai G, Huang B (2009) *J Phys Chem C* 113(37):16394
16. Tong ZW, Yang D, Sun YY (2015) *Phys Chem Chem Phys* 17(18):12199
17. Wang M, Han J, Xiong H (2015) *Langmuir* 31(22):6220
18. Wang X, Utsumi M, Yang Y (2015) *Appl Surf Sci* 325:1
19. Pan L, Wang S, Xie J (2016) *Nano Energy* 28:296
20. Xie J, Yang Y, He H (2015) *Appl Surf Sci* 355:921
21. Liu R, Hu P, Chen S (2012) *Appl Surf Sci* 258(24):9805
22. Teng W, Li X, Zhao Q (2013) *J Mater Chem A* 1(32):9060
23. Yang ZM, Huang GF, Huang WQ (2014) *J Mater Chem A* 2(6):1750
24. Thomas M, Ghosh SK, George KC (2002) *Mater Lett* 56(4):386
25. Pelavin M, Hendrickson DN, Hollander JM (1970) *J Phys Chem* 74(5):1116
26. Zhang H, Wang G, Chen D (2008) *Chem Mater* 20(20):6543
27. Li Y, Yu L, Li N (2015) *J Colloid Interface Sci* 450:246
28. Serpone N, Maruthamuthu P, Pichat P (1995) *J Photochem Photobiol A* 85(3):247

Publisher's Note Springer Nature remains neutral with regard to jurisdictional claims in published maps and institutional affiliations.

Affiliations

Lu Zhang¹ · Deyou Yu¹ · Minghua Wu^{1,2} · Junxiong Lin¹

¹ Engineering Research Center for Eco-Dyeing and Finishing of Textile, Ministry of Education, Zhejiang Sci-Tech University, Hangzhou 310018, People's Republic of China

² Key Laboratory of Advanced Textile Materials & Manufacturing Technology, Ministry of Education,

Zhejiang Sci-Tech University, Hangzhou 310018, People's Republic of China